Transient Variability In Vapor Intrusion And The Factors That Influence It

Jonathan G. V. Ström,[†] Yijun Yao,[‡] and Eric M. Suuberg[*,†]

†*Brown University, School of Engineering, Providence, RI, USA*

‡*Zhejiang University, Hangzhou, China*

E-mail: eric_suuberg@brown.edu

Abstract

Introduction

Long term vapor intrusion (VI) studies in both residential and larger commercial structures have raised concerns regarding significant observed transient behavior in indoor air contaminant concentrations.[1–7] VI involves the migration of volatilizing contaminants from soil, groundwater or other subsurface sources into overlying structures. VI has been a recognized problem for some time, but many aspects remain poorly understood, particularly with respect to the causes of large temporal transients in indoor air concentrations. There is uncertainty within the VI community regarding how to best develop sampling strategies to address this problem.[1,3,8]

Results from a house operated by Arizona State University (ASU) near Hill AFB in Utah, an EPA experimental house in Indianapolis, IN and a large warehouse at the Naval Air Station (NAS) North Island, CA have all shown significant transient variations in indoor

air contaminant concentrations. All were outfitted with sampling and monitoring equipment that allowed tracking temporal variation in indoor air contaminant concentrations on time scales of hours. All have shown that these concentrations varied significantly with time - orders of magnitude on the timescale of a day or days.[5,9,10]

In one instance the source of the variation was clearly established during the study; at the ASU house a field drain pipe (or "land drain"), which connected to a sewer system, was discovered beneath the house, and careful isolation of this source led to a clear conclusion that this preferential pathway significantly contributed to observed indoor air contaminant levels and their fluctuations.[10,11] While in this case the issue of a contribution from a preferential pathway was clearly resolved, what it left open was a question of whether existence of such a preferential pathway to an area beneath a structure would always be expected to lead to large fluctuations in indoor air contaminant concentrations.

Similarly, a sewer pipe has recently been suggested to be a source of the contaminants found in the EPA Indianapolis house. That site was also characterized by large indoor air contaminant concentration fluctuations.[7,12] Sewer lines have been generally implicated as VI sources at several sites.[12–15] A Danish study estimate that roughly 20% of all VI sites in central Denmark involve significant sewer VI pathways.[16] Thus while the consideration of a role of possible sewer or other preferential pathways is now part of normal good practice in VI site investigation,[1] it is still not known whether the existence of such pathways automatically means that large temporal fluctuations are necessarily to be expected. In some of these cited cases,[13,15] a sewer provided a pathway for direct entry of contaminant into the living space. While potentially important in many cases, this scenario is not further considered here, where the focus is on pathways that deliver contaminant via the soil beneath a structure.

It is, however, now known that even absent a preferential pathway, there may be significant transient variation in indoor air contaminant concentrations at VI sites.[2,4,17] One example is a site at NAS North Island at which no preferential pathways have been identified. Instead, a building at this site is characterized by significant temporal variations in

indoor-outdoor pressure differential.[5] It is believed that this is the origin of the observed indoor air contaminant concentration fluctuations at that site.

This paper investigates the sources of the temporal variation in indoor air contaminant concentrations in both the presence and absence of preferential pathways. In this work, the latter scenarios are referred to as "normal" VI scenarios, in which there is typically a groundwater source of the contaminant. Specifically, we pose the question of just how much variation in indoor air contaminant concentration may be expected at such normal VI sites vs. those characterized by preferential pathways. The conditions required for preferential pathways to become significant contributors to temporal variations in indoor air contaminant concentrations are also explored, and the consequences for sampling strategies are also discussed.

Methods

Statistical Analysis Of Field Data

To begin to characterize transient behavior in indoor air contaminant concentrations, actual datasets are analyzed to establish common levels of variability at VI sites. For this purpose, the datasets from the ASU house in Utah, the EPA Indianapolis site and North Island NAS were chosen for analysis. This paper relies on statistical analysis of published field data, and readers are referred to the original works for details regarding data acquisition.[3,5,7,9,10]

The ASU house data were obtained over a period of a few years. During part of this time, controlled pressure method (CPM) tests were being conducted, in which the house was underpressurized to an extent greater than that characterizing "normal" operation. This caused greater than normal advective flow from the subsurface into the house, thus increasing VI potential.[6,9,18] This period of CPM testing is considered separately from the otherwise "natural" VI conditions in the analysis. Likewise, the existence of a preferential pathway at the ASU house needs to be considered in examining the dataset, noting that

during some of the testing, this pathway was deliberately cut off, resulting in what we have termed "normal" VI conditions in which the main source of contaminant was believed to be groundwater.

The NAS North Island dataset has not (as far as is known) been influenced by a preferential pathway, but the structure there was subject to large internal pressure fluctuations, much more extensive than those typically recorded at the ASU house during normal operations. Additionally, the underlying soil at NAS North Island is sandy and more permeable than that at the ASU site, which, as will be shown, contributes to the indoor air contaminant concentrations being more sensitive to pressure fluctuations.[5]

Likewise, the Indianapolis site investigation spanned a number of years and periodically included the testing of a sub-slab depressurziation system (SSD). The goal of the SSD testing was to mitigate the VI risk by drastically depressurizing the sub-slab area underneath the house, preventing the contaminants from entering the structure above. Only the period before the installation of this system was considered in the present analysis. It is likely a sewer line beneath the structure acted as a preferential pathway,[12] however at no point was this preferential pathway removed, making it difficult to assess how significant the role of the preferential pathway was at this site. Regardless of this it is of interest to consider the data from this site due to how extensive and complete the data collection was.

The typical variation in indoor air contaminant concentrations with time will first be considered below in the case of the ASU house during "natural", (i.e. non-CPM conditions), in the case of the NAS North Island site over the entire available dataset, and for the Indianapolis case we consider the variations before the installation of the SSD system. The deviations in indoor air concentration from the mean TCE (and Chloroform and PCE at the Indianapolis site) values, as well as the indoor-outdoor pressure differentials associated with these concentrations were examined. Both univariate and bivariate kernel density estimations (KDE) were constructed. KDE is a technique that estimates the probability distribution of a random variable(s) by using multiple kernels, or weighting functions, and

in this case, Gaussian kernels are used to create the KDEs. This means that it is presumed that the variables of interest (i.e., indoor air contaminant concentrations and indoor-outdoor pressure differentials, as sampled) are normally distributed around mean values (and that there are statistical fluctuations associated with each sampling event). In this instance, the scipy statistical package was used to construct the KDEs, assuming a bandwidth parameter determined by Scott's rule. The distributions of the individual parameters and the relationship between them will be examined using the KDE method.

Modeling Work

In addition to examining the actual field data, a previously described three -dimensional computational fluid dynamics model of a generic VI impacted house was used to elucidate certain aspects of the processes. This model was implemented in a finite element solver package, COMSOL Multiphysics. In the present work, there has been an addition of a preferential pathway to the "standard" model that has been described before in publications by this group.[19–21] As in the earlier studies, only the vadose zone soil domain is directly modeled.

The modeled structure is assumed to have a 10x10 m foundation footprint, with the bottom of the foundation slab lying 1 m below ground surface (bgs), simulating a house with a basement. The indoor air space is modeled as a continuously stirred tank (CST)[1] and all of the contaminant entering the house is assumed to enter with soil gas through a 1 cm wide crack located between the foundation walls and the foundation slab around the perimeter of the house. All of the contaminant leaving the indoor air space is assumed to do so via air exchange with the ambient. The indoor control volume is assumed to consist of only of the basement, assumed as having a total volume of 300 m^3. Clearly different assumptions could be made regarding the structural features and the size of the crack entry route, but for present purposes, this is unimportant as the intent is only to show for "typical" values what the influence of certain other features can be.

The modeled surrounding soil domain extends 5 meters from the perimeter of the house, and is assumed to consist of sandy loam (except as noted). Directly beneath the foundation slab, there is assumed to be a 30 cm (one foot) thick gravel layer, except in certain cases where this sub-base material is assumed to be the same as the surrounding soil (termed a "uniform" soil scenario).

Where relevant The preferential pathway is modeled as a 10 cm (4") pipe that exits into the gravel sub-base beneath the structure. The air in the pipe is assumed to be contaminated with TCE at a vapor concentration equal to the vapor in equilibrium with the groundwater contaminant concentration below the structure, modified by a scaling factor χ, allowing the contaminant concentration in the pipe to be parameterized.

The groundwater beneath the structure is assumed to be homogeneously contaminated with trichloroethylene (TCE) as a prototypical contaminant. The groundwater itself is not modeled, as the bottom of the model domain is defined by the top of the water table. The ground surface and the pipe are both assumed to be sources of air to the soil domain. Both are assumed to be at reference atmospheric pressure.

Vapor transport in the soil is governed by Richard's equation, a modified version of Darcy's Law, taking the variability of soil moisture in the vadose zone into account.[22] The van Genuchten equations are used to predict the soil moisture content and thus the effective permeability of the soil.[23] The effective diffusivity of contaminant in soil is calculated using the Millington-Quirk model.[24] The transport of vapor contaminant in the soil is assumed to be governed by the advection-diffusion equation, in which either advection or diffusion may dominate depending upon position and particular circumstances. The equations and the boundary conditions are given in Table 1.

Table 1: Governing equations, boundary conditions & model input parameters. (See below for table of nomenclature).

(a) Governing equations

Unsteady-CSTR	$V\frac{du}{dt} = \int_{A_{\text{ck}}} j_{\text{ck}} dA - uA_eV$
Richard's equation	$\nabla \cdot \rho\Big(-\frac{\kappa_s}{\mu} k_r \nabla p\Big) = 0$
Millington-Quirk	$D_{\text{eff}} = D_{\text{air}}\frac{\theta_g^{10/3}}{\theta_t^2} + \frac{D_{\text{water}}}{K_H}\frac{\theta_w^{10/3}}{\theta_t^2}$
Advection-diffusion equation	$\frac{\partial}{\partial t}\Big(\theta_w c_w + \theta_g c\Big) = \nabla(D_{\text{eff}} \cdot \nabla c) - \vec{u} \cdot \nabla c$
van Genuchten equations	$\text{Se} = \frac{\theta_w - \theta_r}{\theta_t - \theta_r} = [1 + \lvert\alpha z\rvert^n]^{-m}$ $\theta_g = \theta_t - \theta_w$ $k_r = (1 - \text{Se})^l[1 - (\text{Se}^{-m})^m]^2$ $m = 1 - 1/n$

(b) Boundary conditions

Boundary	**Richard's equation**	**Advection-diffusion equation**
At foundation crack	$p = p_{\text{in/out}}$ (Pa)	$j_{\text{ck}} = \frac{uc}{1-\exp(uL_{\text{slab}}/D_{\text{air}})}$
At groundwater source	N/A	$c = c_{\text{gw}}K_H$ (μg/m^3)
At ground surface	$p = 0$ (Pa)	$c = 0$ (μg/m^3)
Exit of preferential pathway	$p = 0$ (Pa)	$c = c_{\text{gw}}K_H\chi$ (μg/m^3)

(c) Soil & gravel properties[25–27]

Soil	Permeability (m^2)	Density (kg/m^3)	θ_s	θ_r	α (1/m)	n
Gravel	$1.3 \cdot 10^{-9}$	1680	0.42	0.005	100	3.1
Sandy Loam	$5.9 \cdot 10^{-13}$	1460	0.39	0.039	2.7	1.4

(d) Trichloroethylene (diluted in air) properties[26,27]

D_{air} (m^2/h)	D_{water} (m^2/h)	Density (kg/m^3)	Viscosity (Pa $\cdot$ s)	K_H	M (g/mol)
$2.47 \cdot 10^{-2}$	$3.67 \cdot 10^{-6}$	1.614	$1.86 \cdot 10^{-5}$	0.403	131.39

(e) Building properties

V_{base} (m^3)	L_{slab} (cm)	A_e (1/hr)
300	15	0.5

Results & Discussion

Statistical Analysis of Field Data

The pressure difference between the indoor and outdoor/ambient ($p_{\text{in/out}}$) is an important driving force in VI, drawing in (or preventing) contaminants from entering a structure.

Figure 1: Distributions of indoor/outdoor pressure differences (top row), and its correlation with indoor air contaminant concentrations (middle rows), and air exchange rate (bottom row), at three different VI sites - ASU house, Indianapolis site, and North Island NAS.

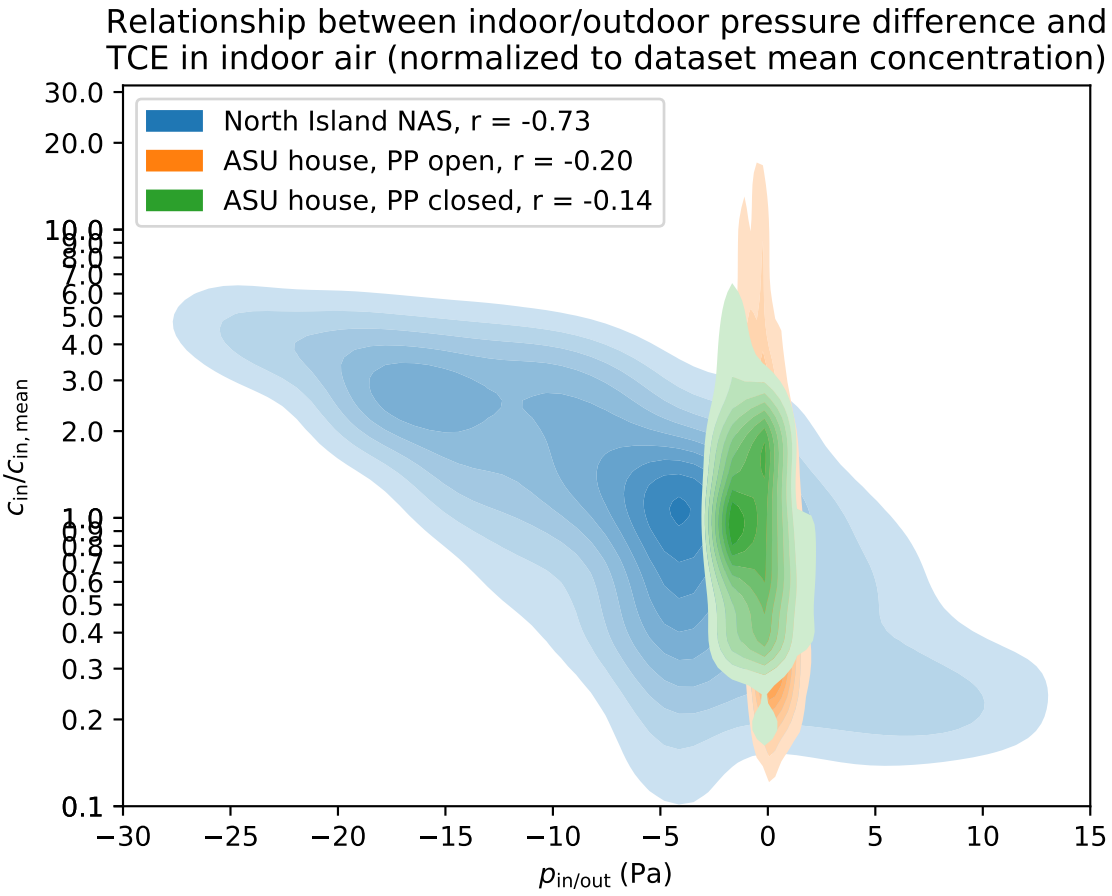

Table 2: 5th and 95th percentile values of $p_{\text{in/out}}$ and $c_{\text{in}}/c_{\text{in,mean}}$ in Figure 1.

	North Island NAS		**ASU house PP Open**		**ASU House PP Closed**	
Percentile	5th	95th	5th	95th	5th	95th
$p_{\text{in/out}}$ (Pa)	-19.9	7.4	-1.4	2.1	-2.1	2.27
$c_{\text{in}}/c_{\text{in,mean}}$	4.1	0.2	13.5	0.2	3.3	0.4

Changes in $p_{\text{in/out}}$ is also a dynamic and fast process, impacting VI more rapidly than e.g. fluctuations in groundwater depth or contaminant concentration does; these processes may take weeks or even months to impact the overlying structure. Therefore it is reasonable to assume that the temporal variability in indoor air contaminant concentration c_{in} may be driven by changes in $p_{\text{in/out}}$.

We examine the relationship between $p_{\text{in/out}}$ and c_{in} by constructing the two-dimensional kernel density estimation (KDE) plots seen in Figure 1. The KDE plot allows us to view the distribution of $p_{\text{in/out}}$ and c_{in}, and how well these correlate. For this analysis we consider two VI sites, North Island NAS, and the ASU house, with the ASU house dataset divided up into two periods, before and after the land drain (called preferential pathway (PP) from here on) had been closed. The preferential pathway significantly impacted the ASU house to such an extent that these two periods can essentially be considered as two different VI sites, and allowing us to examine the effect it had.

In Figure 1 c_{in} is normalized to the mean $c_{\text{in,mean}}$ of each dataset, allowing us to compare the impact $p_{\text{in/out}}$ had on c_{in}. A value of 10 on the y-axis indicate that c_{in} is 10 times greater than the mean here, and 0.1 indicate that it is one tenth of the mean. The Pearson's r between $p_{\text{in/out}}$ and c_{in} for each dataset is shown in the legend.

An interesting aspect of the North Island NAS site is that $p_{\text{in/out}}$ varies so significantly here, with the 5th and 9th percentile $p_{\text{in/out}}$ -19.9 and 7.4 Pa respectively. This may be contrasted with 5th and 95th percentile $p_{\text{in/out}}$ at the ASU house: -1.4 and 2.1 Pa (PP open), and -2.1 and 2.27 Pa (PP closed).

The large (roughly one order of magnitude) under- and overpressurization of the North Island NAS site leads to roughly a one order magnitude increase and decrease from the mean c_{in}. Combined with $r = -0.73$, it is quite clear that at this site $p_{\text{in/out}}$ largely determines c_{in} (there is still variability in c_{in} for a given $p_{\text{in/out}}$, which we address later). This is the same principle that governs the controlled pressure method (CPM) concept.

Turning to the ASU house datasets, we see a quite different situation. Here the variability of c_{in} is just as large, or even larger than at North Island NAS, yet the $p_{\text{in/out}}$ varies far less. At first glance it may seem like the c_{in} values for the periods when the PP is open and closed respectively are relatively comparable, but the 5th and 95th percentiles values of differ significantly $c_{\text{in}}/c_{\text{in,mean}}$ as may be seen in Table 2.

It is clear that the PP dramatically increases the house's sensitivity to $p_{\text{in/out}}$, and the

site is fundamentally different during the period when the PP was open. Yet, the magnitude of change in c_{in} is far greater than the change in $p_{\text{in/out}}$, leading to the conclusion that it is not just increased flow rates into the structure that causes this, but there must also be an increased amount of contaminant as well as a much larger spatial variability in the sub-base. This is a topic that we will return to later.

The magnitude of change in c_{in} when the PP is closed is more in line with the magnitude of change in $p_{\text{in/out}}$, but there is still more variability than one would expect. We hypothesize that this is largely due to fluctuations in air exchange rate, which we will examine later.

Change In Indoor Air Contaminant Concentration Over Time

Figure 2: (1D is 1 day, 2W is 2 weeks, and 3M is 3 months).

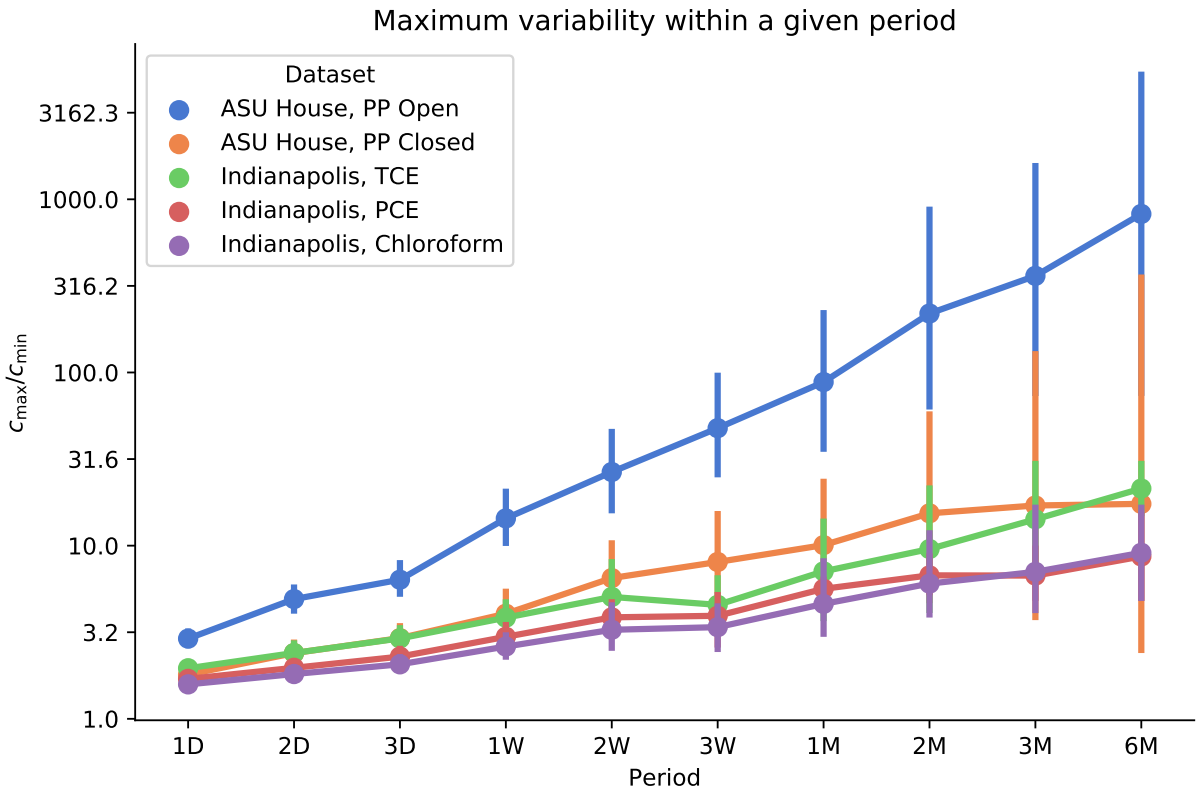

So far we have discussed how the relationship between c_{in} and $p_{\text{in/out}}$, and how significantly c_{in} may vary at a site. But this tells us little about how much variability in c_{in} may

be expected over time. For this analysis we turn to the ASU house data (PP open/closed considered separately again), and another well-studied VI site, the Indianapolis site in Indiana. Both of these sites collected high frequency c_{in} samples over a significant periods and are therefore suitable. Furthermore, at Indianapolis site the c_{in} of three different contaminants, Chloroform, Trichloroethylene (TCE), and Tetrachloroethylene (PCE) were collected, allowing us to see if there is any difference in the variability of each. The North Island NAS dataset only spans a few days, and is therefore excluded from this analysis.

To demonstrate how significantly c_{in} can vary across time, we calculate at the quotient of the maximum and minimum c_{in} (denoted as $c_{\max}/c_{\min}$) over a given time period. I.e. if c_{in} samples were collected every four hours over a period of a year, and the data is resampled on a daily basis, then $c_{\max}/c_{\min}$ is returned for within each day, giving 365 data points. Resampling periods of one, two, three, days, weeks, and months are chosen and Figure 2 shows the result of this analysis.

As one might expect, the longer the resampling period, the larger the maximum variability is, spanning from less than a threefold difference, to two to three orders of magnitude. That such a large variability is observed when the resampling time approaches the length of the entire datasets is hardly surprising, nor is it surprising that the variability is much more significant when the preferential pathway was open than closed. What may be surprising is that absent a preferential pathway such as the one at the ASU house, it may take a few weeks before an order of magnitude maximum variability is reached. The most significant result of this analysis is that the maximum variability is quite small across a few days, suggesting that e.g. 24-hour passive samplers will resolve the daily temporal variability in c_{in} well ($c_{\max}/c_{\min} \approx 1.5$) and that a sampling frequency greater than a few days may yield little extra information. There is also little difference between maximum variability of c_{in} the ASU house (when the PP is closed), and the three contaminants at the Indianapolis site.

Figure 3: Boxplot of attenuation from subslab at the ASU house site. The box shows the quartiles of the distribution, the whiskers the extent of the distribution, and diamonds are points that are considered outlier.

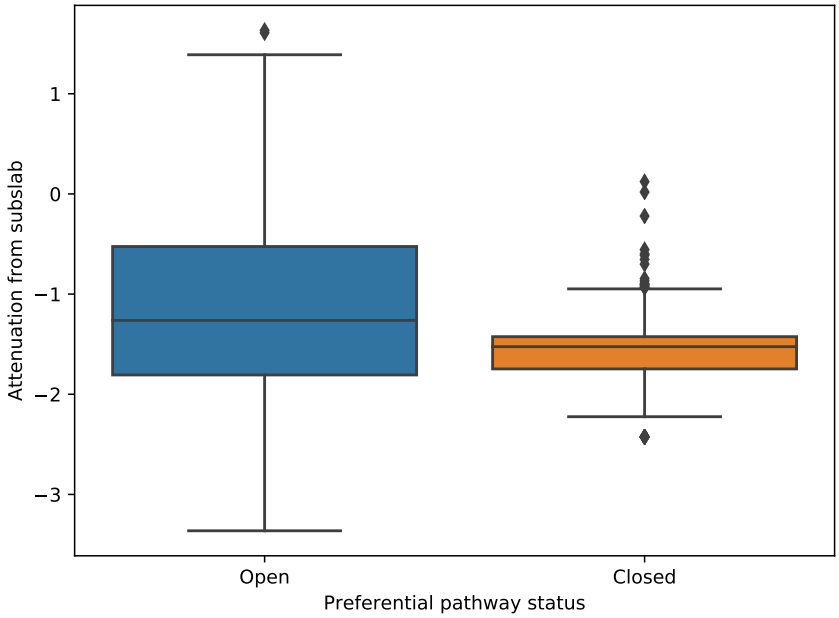

Variability Of Attenuation From Subslab

To examine how $p_{\text{in/out}}$ affects the contaminant entry rate it would be most convenient to analyze how $p_{\text{in/out}}$ is correlated with the attenuation from subslab ($\alpha_{\text{subslab}} = c_{\text{in}}/c_{\text{subslab}}$) at a site - in particularly for understanding how the PP at the ASU house affected the site dynamics. By normalizing the c_{in} to c_{subslab} the $p_{\text{in/out}}$ influence on the contaminant availability in the subslab area is mitigated. The c_{subslab} are taken from the soilgas probe labeled as "6" at the ASU house, which is the probe located closest to the preferential pathway, and to a reported breach in the foundation.[11] However, as Figure 3 shows, there are some issues with doing so.

First, we can state that during the period when the preferential pathway was closed, α_{subslab} does not vary that significantly, and is mostly around the EPA recommended α_{subslab} value of 0.03. During the period when the preferential pathway was open, there is considerably more variability, and it is not uncommon for the α_{subslab} to exceed unity.

Even though probe "6" is located in such close proximity to the preferential pathway, and the breach in the foundation, the contaminant concentration 'hotspot' is still missed. This suggests that a preferential pathway may have an extremely localized influence in the subslab region, causing significant spatial variability in c_{subslab}. This shows how difficult it may be to locate a preferential pathway through subslab soilgas sampling.

The large α_{subslab} values (compared to the recommended EPA value of 0.03) can often indicate that there may be indoor sources present a site, which there were none of at the ASU house. Thus, in addition to potentially indicating indoor contaminant sources, large α_{subslab} may also indicate the presence of a preferential pathway.

Influence Of Pressure On Indoor Air Variability

Figure 4: Simulated cases

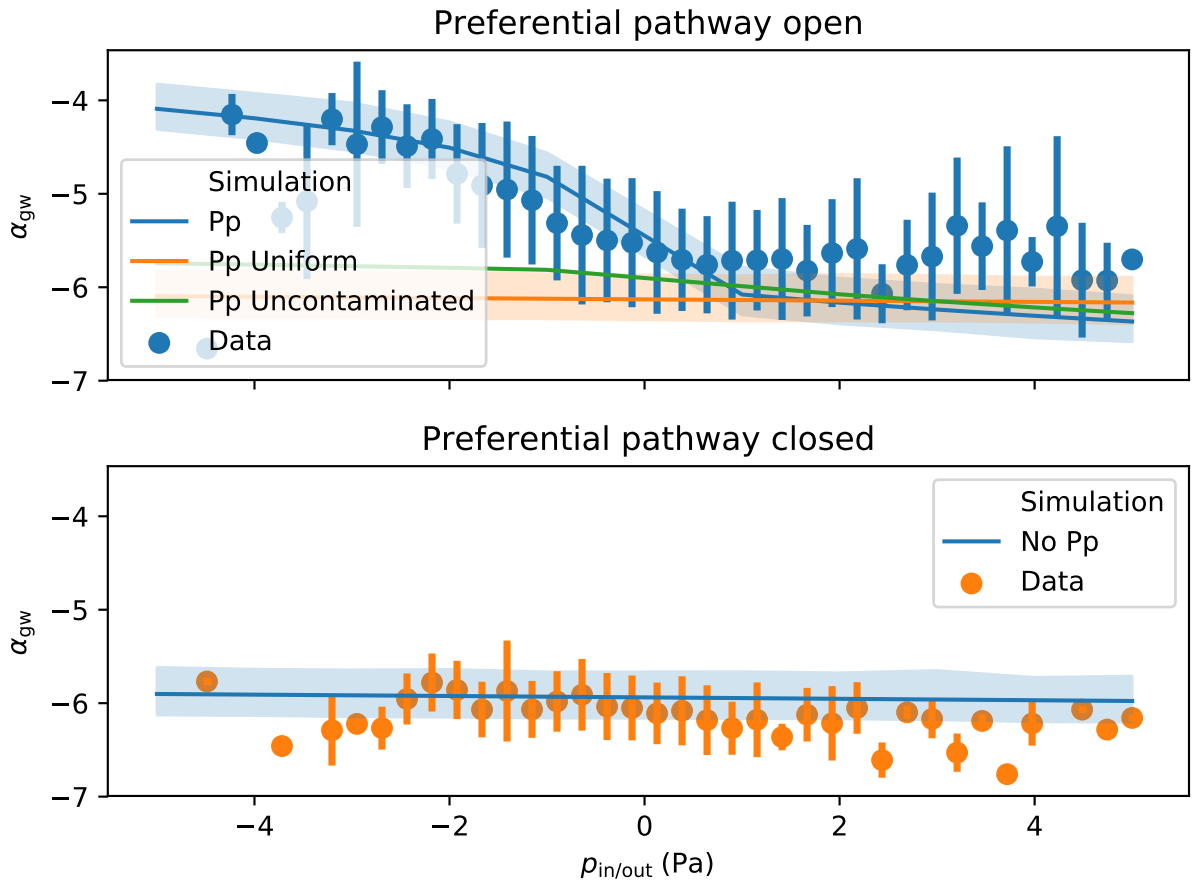

To examine the role that $p_{\text{in/out}}$ play in determining c_{in} variability (given as attenuation from groundwater vapor source α_{gw} here), we first consider modeling VI scenarios with a constant $A_e = 0.5$ (1/hr) (the mean A_e at the ASU house), and varying $p_{\text{in/out}}$ from 5 to -5 Pa. The first of these scenarios is aimed to be similar to the period when the preferential pathway is open at the ASU house, and thus the modeled preferential pathway is active. In the second scenario, this preferential pathway feature is deactivated, akin to the period when the preferential pathway was closed at the ASU site. And in the third, the preferential pathway is again modeled, but the permeable gravel sub-base is instead assumed consist of the sandy loam, just like the surrounding soil, giving an "uniform soil" scenario. The results of these modeled scearios are then compared to the preferential pathways "open" and "closed" periods from the ASU data, and may be seen in Figure **??**. The data is here binned into evenly spaced bins, with each dot representing the mean α_{gw} and the error bars denote the one standard deviation.

By examining the first scenario (blue) it is readily apparent that the model is able to capture the behavior of the preferential pathway when the structure is depressized ($p_{\text{in/out}} < 0$) but not very well when the house is overpressurized ($p_{\text{in/out}} > 0$). This shows that the preferential pathways acts by increasing advective potential, allowing even relatively small increases in depressurziation dramatically increases the contaminant entry rate into the house. Conversely, when the structure is overpressurized, contaminant entry is more effectively inhibited, leading to diffusion being the more important transport mechanism from the sub-base to the indoor air space, leading to the decrease in α_{gw}. Yet, when $p_{\text{in/out}} > 0$ there is a slight increase in α_{gw} which can be explained by the fact that lower A_e are associated with overpressurazation, leading to an increase in α_{gw},

An interesting contrast to this scenario is third, when the preferential pathway is still present but the permeable gravel sub-base is not. Under these conditions, there is almost increase in advective transport as the impermeable sub-base effectively inhibits this. This leads to the conclusion that a unless there is some way for a preferential pathway to effectively

communicate between the sub-base region (or wherever the preferential pathway is), then it is unlikely to find the dramatic effect observed at the ASU house.

Lastly, we consider the second scenario, where there is no preferential pathway present (but there is a permeable gravel sub-base). Here the general (weak) trend of increased α_{gw} with increase depressurziation is captured, but none of the variability is captured. There is inadequate potential for advective transport and thus $p_{\text{in/out}}$ does not significantly increase the contaminant entry rate. Furthermore, the seemingly random variability is not captured. Clearly, the A_e fluctations must be incorporated into the modeling methodoly to more accurately predict the variability in α_{gw}.

Attenuation To Subslab

Acknowledgement

This project was supported by grant ES-201502 from the Strategic Environmental Research and Development Program and Environmental Security Technology Certification Program (SERDP-ESTCP).

References

(1) U.S. Environmental Protection Agency, OSWER Technical Guide for Assessing and Mitigating the Vapor Intrusion Pathway From Subsurface Vapor Sources To Indoor Air. `https://www.epa.gov/sites/production/files/2015-09/documents/oswer-vapor-intrusion-technical-guide-final.pdf`, 00005.

(2) Folkes, D.; Wertz, W.; Kurtz, J.; Kuehster, T. Observed Spatial and Temporal Distributions of CVOCs at Colorado and New York Vapor Intrusion Sites. *29*, 70–80, 00048.

(3) Holton, C.; Luo, H.; Dahlen, P.; Gorder, K.; Dettenmaier, E.; Johnson, P. C. Temporal

Variability of Indoor Air Concentrations under Natural Conditions in a House Overlying a Dilute Chlorinated Solvent Groundwater Plume. *47*, 13347–13354, 00028.

(4) Johnston, J. E.; Gibson, J. M. Spatiotemporal Variability of Tetrachloroethylene in Residential Indoor Air Due to Vapor Intrusion: A Longitudinal, Community-Based Study. *24*, 564, 00018.

(5) Hosangadi, V.; Shaver, B.; Hartman, B.; Pound, M.; Kram, M. L.; Frescura, C. High-Frequency Continuous Monitoring to Track Vapor Intrusion Resulting From Naturally Occurring Pressure Dynamics. *27*, 9–25, 00001.

(6) McHugh, T.; Loll, P.; Eklund, B. Recent Advances in Vapor Intrusion Site Investigations. *204*, 783–792, 00005.

(7) U.S. Environmental Protection Agency, Assessment of Mitigation Systems on Vapor Intrusion: Temporal Trends, Attenuation Factors, and Contaminant Migration Routes under Mitigated And Non-Mitigated Conditions. 00002.

(8) Johnson, P. C.; Holton, C. W.; Guo, Y.; Dahlen, P.; Luo, E. H.; Gorder, K.; Dettenmaier, E.; Hinchee, R. E. Integrated Field-Scale, Lab-Scale, and Modeling Studies for Improving Our Ability to Assess the Groundwater to Indoor Air Pathway at Chlorinated Solvent-Impacted Groundwater Sites. 00003.

(9) Holton, C. W. Evaluation of Vapor Intrusion Pathway Assessment Through Long-Term Monitoring Studies. `https://repository.asu.edu/attachments/150778/content/Holton_asu_0010E_15040.pdf`, 00003.

(10) Guo, Y. Vapor Intrusion at a Site with an Alternative Pathway and a Fluctuating Groundwater Table. `https://repository.asu.edu/items/36435`, 00001.

(11) Guo, Y.; Holton, C.; Luo, H.; Dahlen, P.; Gorder, K.; Dettenmaier, E.; Johnson, P. C.

Identification of Alternative Vapor Intrusion Pathways Using Controlled Pressure Testing, Soil Gas Monitoring, and Screening Model Calculations. *49*, 13472–13482, 00019.

(12) McHugh, T.; Beckley, L.; Sullivan, T.; Lutes, C.; Truesdale, R.; Uppencamp, R.; Cosky, B.; Zimmerman, J.; Schumacher, B. Evidence of a Sewer Vapor Transport Pathway at the USEPA Vapor Intrusion Research Duplex. *598*, 772–779, 00007.

(13) Pennell, K. G.; Scammell, M. K.; McClean, M. D.; Ames, J.; Weldon, B.; Friguglietti, L.; Suuberg, E. M.; Shen, R.; Indeglia, P. A.; Heiger-Bernays, W. J. Sewer Gas: An Indoor Air Source of PCE to Consider During Vapor Intrusion Investigations. *33*, 119–126, 00022.

(14) Roghani, M.; Jacobs, O. P.; Miller, A.; Willett, E. J.; Jacobs, J. A.; Viteri, C. R.; Shirazi, E.; Pennell, K. G. Occurrence of Chlorinated Volatile Organic Compounds (VOCs) in a Sanitary Sewer System: Implications for Assessing Vapor Intrusion Alternative Pathways. *616-617*, 1149–1162, 00002.

(15) Riis, C. E.; Christensen, A. G.; Hansen, M. H.; Husum, H.; Terkelsen, M. Vapor Intrusion through Sewer Systems: Migration Pathways of Chlorinated Solvents from Groundwater to Indoor Air. Seventh International Conference on Remediation of Chlorinated and Recalcitrant Compounds. 00012.

(16) Nielsen, K. B.; Hvidberg, B. Remediation Techniques for Mitigating Vapor Intrusion from Sewer Systems to Indoor Air. *27*, 67–73, 00002.

(17) Brenner, D. Results of a Long-Term Study of Vapor Intrusion at Four Large Buildings at the NASA Ames Research Center. *60*, 747–758, 00003.

(18) McHugh, T. E.; Beckley, L.; Bailey, D.; Gorder, K.; Dettenmaier, E.; Rivera-Duarte, I.; Brock, S.; MacGregor, I. C. Evaluation of Vapor Intrusion Using Controlled Building Pressure. *46*, 4792–4799, 00037.

(19) Shen, R.; Pennell, K. G.; Suuberg, E. M. Influence of Soil Moisture on Soil Gas Vapor Concentration for Vapor Intrusion. *30*, 628–637, 00015 WOS:000325689400005.

(20) Yao, Y.; Wang, Y.; Zhong, Z.; Tang, M.; Suuberg, E. M. Investigating the Role of Soil Texture in Vapor Intrusion from Groundwater Sources. *46*, 776–784, 00003.

(21) Yao, Y.; Mao, F.; Ma, S.; Yao, Y.; Suuberg, E. M.; Tang, X. Three-Dimensional Simulation of Land Drains as a Preferential Pathway for Vapor Intrusion into Buildings. *46*, 1424–1433, 00002.

(22) Richards, L. A. Capillary Conduction of Liquids through Porous Mediums. *1*, 318–333, 05183.

(23) van Genuchten, M. T. A Closed-Form Equation for Predicting the Hydraulic Conductivity of Unsaturated Soils. *44*, 892–898, 00004.

(24) Millington, R. J.; Quirk, J. P. Permeability of Porous Solids. *57*, 1200, 01808.

(25) Dan, H.-C.; Xin, P.; Li, L.; Li, L.; Lockington, D. Capillary Effect on Flow in the Drainage Layer of Highway Pavement. *39*, 654–666, 00007.

(26) Abreu, L. D. V.; Schuver, H. Conceptual Model Scenarios for the Vapor Intrusion Pathway. `https://www.epa.gov/sites/production/files/2015-09/documents/vi-cms-v11final-2-24-2012.pdf`, 00010.

(27) U.S. Environmental Protection Agency, Users's Guide For Evaluating Subsurface Vapor Intrusion Into Buildings. `https://www.epa.gov/sites/production/files/2015-09/documents/2004_0222_3phase_users_guide.pdf`, 00000.